Rhodocenium Complexes Bearing the 1,2,3-Tri-*tert*-butylcyclopentadienyl Ligand: Redox-Promoted Synthesis and Mechanistic, Structural and Computational Investigations

Bernadette T. Donovan-Merkert,* C. Reid Clontz, Leslie M. Rhinehart, Howard I. Tjiong, and Clifford M. Carlin

Department of Chemistry, The University of North Carolina at Charlotte, 9201 University City Boulevard, Charlotte, North Carolina 28223-0001

Thomas R. Cundari*

Department of Chemistry, University of Memphis, Memphis, Tennessee 38152

Arnold L. Rheingold* and Ilia Guzei

Department of Chemistry, University of Delaware, Newark, Delaware 19716

Received September 2, 1997

Single-electron oxidation of rhodium complexes containing the 1,2,3,5-η-penta-2,4-dienediyl ligand was conducted by electrochemical and chemical means. In all cases, rhodocenium complexes bearing the η^5-1,2,3-tri-*tert*-butylcyclopentadienyl ligand were produced in good yield. The results of single-crystal X-ray diffraction studies revealed the solid-state structures of $[Rh(\eta^5\text{-}C_5H_5)(\eta^5\text{-}C_5{}^tBu_3H_2)][PF_6]$ (**10a**$^+$) and $[Rh(\eta^5\text{-}C_5H_5)(\eta^5\text{-}C_5{}^tBu_3H_2)][BF_4]$ (**10b**$^+$). The steric strain in these molecules is apparently relieved by in-plane distortions of the bond lengths and angles of the tri-*tert*-butylcyclopentadienyl ligand. The results of a deuterium-labeling study revealed the stereochemistry of the ring-closure reaction. Computational studies using the PM3 semiempirical Hamiltonian suggest that oxidation of the pentadienediyl complexes involves removal of an electron from a molecular orbital centered on the pentadienediyl ligand.

Introduction

Transition-metal, main-group, and f-element complexes bearing cyclopentadienyl ligands with sterically demanding substituents have attracted considerable interest. The syntheses and properties of complexes possessing more than one bulky substituent on a cyclopentadienyl ligand were recently reviewed.[1] Most examples of compounds bearing cyclopentadienyl ligands possessing more than one *tert*-butyl substituent are those which contain 1,3-di- or 1,3,5- tri-*tert*-butylcyclopentadienyl ligands.[2] Reports on the synthesis of the 1,2-di-*tert*-butylcyclopentadienyl ligand and complexes thereof have also appeared.[3]

Hughes and co-workers recently reported the first example of a complex bearing the novel 1,2,3-tri-*tert*-butylcyclopentadienyl ligand.[4] The crystallographically characterized[4b] rhodocenium complex **5a**$^+$ (Scheme 1) was synthesized by a metal-promoted ring-expansion reaction of tri-*tert*-butylvinylcyclopropene **1a**. After cleavage of the vinylcyclopropene ring, the initially formed pentadienediyl complex **2a** was converted to its indenyl derivative **3a**. The conversion of **3a** to η^4-cyclopentadiene complex **4a** was accomplished by heating the product in benzene solution or by chromatography on cold Florisil. **4a** reacted with a variety of reagents to produce **5a**$^+$ in good yield. An analogous reaction starting with deuterium-labeled **1b** resulted in **5b**$^+$, thereby establishing the stereochemistry of the ring-closure reaction.

(1) (a) Okuda, J. *Top. Curr. Chem.* **1992**, *160*, 97. (b) Janiak, C.; Schumann, H. *Adv. Organomet. Chem.* **1991**, *33*, 291.

(2) For example, see: (a) Jibril, I.; Abu-Nimreh, O. *Synth. React. Inorg. Met.-Org. Chem.* **1996**, *26*, 1409. (b) Sofield, C.; Anderson, R. A. *J. Organomet. Chem.* **1995**, *501*, 271. (c) Schneider, J. J.; Specht, U. *Z. Naturforsch., B* **1995**, *50*, 684. (d) Sitzmann, H.; Wolmershaeuser, G. *Chem. Ber.* **1994**, *127*, 1335. (e) Cotton, J. D.; Byriel, K. A.; Kennard, C. H.; Scheck, T.; Lynch, D. E. *J. Organomet. Chem.* **1993**, *462*, 243. (f) Scheer, M.; Schuster, K.; Becker, U.; Krug, A.; Hasrtung, H. *J. Organomet. Chem.* **1993**, *460*, 105. (g) Boehme, U.; Langhof, H. *Z. Kristallogr.* **1993**, *206*, 281. (h) Boese, R.; Blaeser, D.; Kuhn, N.; Stubenrauch, S. *Z. Kristallogr.* **1993**, *205*, 282. (i) Reddy, A. C.; Jemmis, E. D.; Scherer, O. J.; Winter, R.; Heckmann, G.; Wolmershaeuser, G. *Organometallics* **1992**, *11*, 3894. (j) Schneider, J. J.; Krueger, C. *Chem. Ber.* **1992**, *125*, 843. (k) Knyazhanskii, S. Y.; Lobkovskii, E. B.; Bulychev, B. M.; Bel'skii, V. K.; Soloveichik, G. L. *J. Organomet. Chem.* **1991**, *419*, 311. (l) Bel'skii, V. K.; Strel'tsova, N. R.; Gun'ko, Y. K.; Knyazhanskii, S. Y.; Bulychev, B. M.; Soloveichik, G. L. *Metalloorg. Khim.* **1991**, *4*, 1139. (m) Scheer, M.; Schuster, K.; Schenzel, K.; Herrmann, E.; Jones, P. G. *Z. Anorg. Allg. Chem.* **1991**, *600*, 109. (n) Recknagel, A.; Knoesel, F.; Gornitzka, H.; Noltmeyer, M.; Edelmann, F. T.; Behrens, U. *J Organomet. Chem.* **1991**, *417*, 363. (o) Okuda, J. *J. Organomet. Chem.* **1990**, *385*, C39. (p) Is this just the ligand? Sitzmann, H. *Z. Naturforsch., B* **1989**, *44*, 1293. (q) Jutzi, P.; Dickbreder, R. *J. Organomet. Chem.* **1989**, *373*, 301.

(3) (a) Hughes, R. P.; Lomprey, J. R.; Rheingold, A. L.; Yap, G. P. A. *J. Organomet. Chem.* **1996**, 517, 63. (b) Hughes, R. P.; Lomprey, J. R.; Rheingold, A. L.; Haggerty, B. S.; Yap, G. P. A. *J. Organomet. Chem.* **1996**, *517*, 89. (c) Hughes, R. P.; Lomprey, J. R. *Inorg. Chim. Acta* **1995**, *240*, 653. (d) Hughes, R. P.; Kowalski, A. S.; Lomprey, J. R.; Rheingold, A. L. *Organometallics* **1994**, *13*, 2691.

(4) (a) Donovan, B. T.; Hughes, R. P.; Trujillo, H. A. *J. Am. Chem. Soc.* **1990**, *112*, 7076. (b) Donovan, B. T.; Hughes, R. P.; Trujillo, H. A.; Rheingold, A. L. *Organometallics* **1992**, *11*, 64.

S0276-7333(97)00773-5 CCC: $15.00
Publication on Web 03/31/1998

Scheme 1

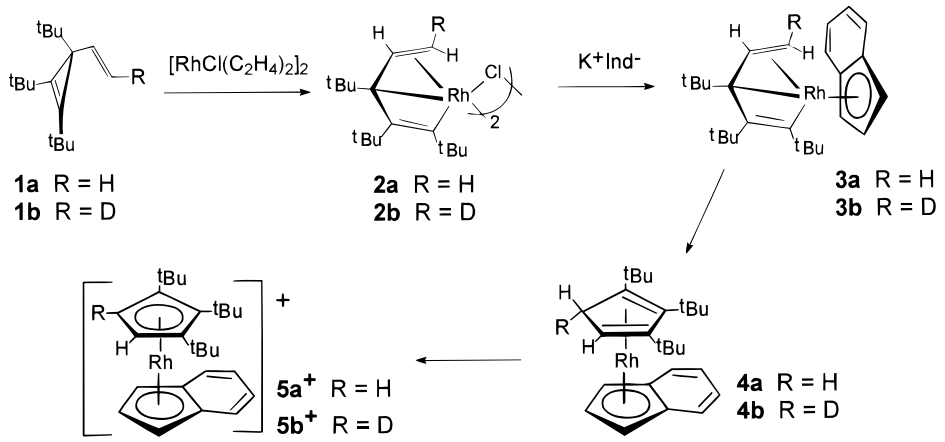

Interestingly, other related rhodium pentadienediyl compounds did not convert to complexes bearing the 1,2,3-tri-*tert*-butylcyclopentadienyl ligand.[5–7] As shown in eq 1, chloride-bridged dimer **2a** converted to η^4-

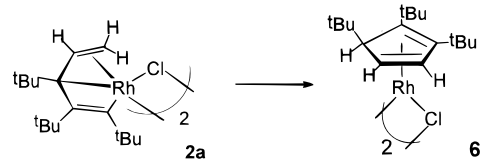

(Eq. 1)

cyclopentadiene compound **6** on prolonged standing in methylene chloride solution.[5] Pentamethylcyclopentadienyl derivative **7** (eq 2) converted to η^4-cyclobutadienyl

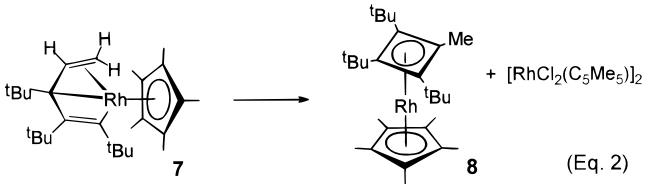

(Eq. 2)

compound **8** (plus $[Rh(C_5Me_5)Cl_2]_2$) on standing in halogenated solvents.[6] Cyclopentadienyl derivative **9a** (eq 3) did not react when heated in refluxing toluene

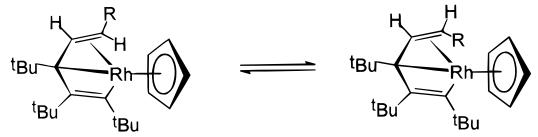

(Eq. 3)

9a R = H
9b R = D

for months, although the syn and anti positions of its deuterium-labeled isotopomer **9b** did exchange after prolonged heating.[7]

Given the current interest in the synthesis, properties, and reactions of substituted cyclopentadienyl ligands, we thought it would be of interest to develop a method of facilitating the conversion of pentadienediyl complexes such as **3**, **7**, and **9** to molecules bearing the η^5-1,2,3-tri-*tert*-butylcyclopentadienyl ligand. In a recent communication,[8] we demonstrated that single-electron chemical or electrochemical oxidation of **9a** rapidly afforded the new rhodocenium complex **10a**$^+$ (see eq 4) and that the conversion **3a**→**5a**$^+$ could also

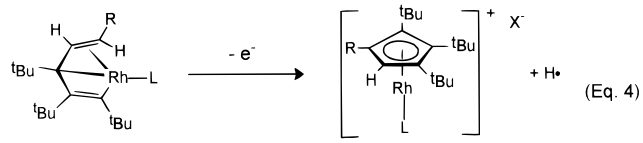

(Eq. 4)

3a L = C_9H_7 R = H
9a L = C_5H_5 R = H
9b L = C_5H_5 R = D
7 L = C_5Me_5 R = H

5a$^+$ L = C_9H_7 R = H X = PF_6
5c$^+$ L = C_9H_7 R = H X = BF_4
10a$^+$ L = C_5H_5 R = H X = PF_6
10b$^+$ L = C_5H_5 R = H X = BF_4
10c$^+$ L = C_5H_5 R = D X = PF_6
11$^+$ L = C_5Me_5 R = H X = PF_6

be carried out using the redox-promoted method. In the present paper, we report the full details of the conversions **9a** → **10a**$^+$ and **3a** → **5a**$^+$, **5c**$^+$, including the results of single-crystal X-ray diffraction studies of **10a**$^+$ and **10b**$^+$. We also show that pentamethylcyclopentadienyl complex **7** undergoes an analogous oxidatively induced transformation to form rhodocenium complex **11**. Computational studies of a model compound using the PM3 semiempirical Hamiltonian suggest that the oxidation process involves removal of an electron from a molecular orbital centered on the pentadienediyl ligand. Finally, we present the results of a deuterium-labeling study which demonstrates the stereochemistry of the oxidatively induced reaction.

Results and Discussion

I. Electrochemistry Investigations of the Pentadienediyl Complexes. (i) The Cyclopentadienyl Complex 9a. Typical cyclic voltammetry (CV) scans of **9a** are shown in Figure 1. The scan represented by the solid line, initiated in the positive potential direc-

(5) Donovan, B. T.; Hughes, R. P.; Kowalski, A. S.; Trujillo, H. A.; Rheingold, A. L. *Organometallics* **1993**, *12*, 1038

(6) Hughes, R. P.; Kowalski, A. S.; Donovan, B. T. *J. Organomet. Chem.* **1994**, *472*, C18.

(7) Donovan, B. T.; Egan, J. W.; Hughes, R. P.; Spara, P. P.; Trujillo, H. A.; Rheingold, A. L. *Isr. J. Chem.* **1990**, *30*, 351.

(8) Donovan-Merkert, B. T.; Tjiong, H. I.; Rhinehart, L. M.; Russell, R. R.; Malik, J. M. *Organometallics* **1997**, *16*, 819.

(9) The ratio (i_{p_a}/i_{p_c})of the peak currents of the anodic (i_{p_a}) and cathodic (i_{p_c}) portions of wave B varies with scan rate. For example, at 200 mV/s, the scan rate employed in the voltammograms of Figure 1, i_{p_a}/i_{p_c} is 0.80 but at 1000 mV/s the ratio is 0.97. This indicates that the product generated during the cathodic process of wave B undergoes a homogeneous reaction whose rate is competitive with the time scale of the slower scan experiment.[10] We are currently investigating the consequences of this homogeneous reaction.

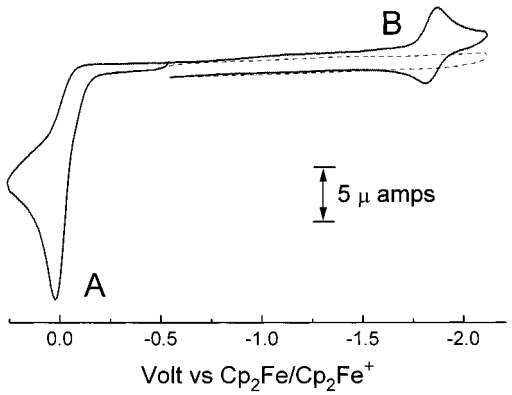

Figure 1. Cyclic voltammetry scans of 0.7 mM **9a** in THF solution. The scan represented by the solid line was initiated in the positive potential direction while the scan represented by the dashed line was initiated in the negative potential direction. The lettered waves arise from the following reactions: (A) **9a** → **10a**$^+$ + e$^-$, (B) **10a**$^+$ + e$^-$ ⇔ **10a**. Conditions: glassy carbon working electrode; scan rate = 200 mV/s.

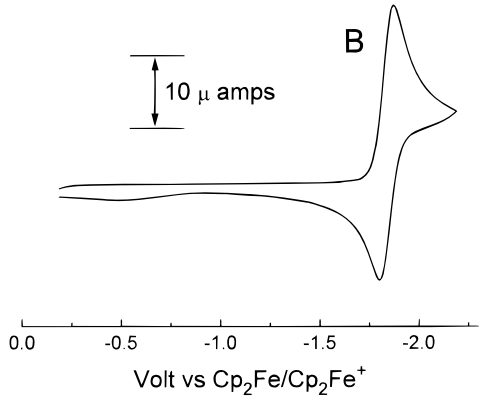

Figure 2. Cyclic voltammetry of 0.7 mM **10a**$^+$ in THF solution. Conditions: glassy carbon working electrode; scan rate = 300 mV/s.

tion, shows the presence of a chemically irreversible oxidation wave labeled A (E_{p_a} = +0.02 V) and a nearly chemically reversible wave labeled B ($E_{1/2}$ = −1.83 V).[9] The chemical irreversibility of wave A persists at a scan rate of 2 V/s, indicating that oxidation of **9a** results in a rapid homogeneous reaction.[10] The product of the reaction was identified as rhodocenium complex **10a**$^+$ by NMR and a single-crystal X-ray diffraction study (vide infra). Wave B appears only when wave A is traversed first and hence is absent in the scan depicted by the dashed line. Additionally, the cathodic portion of wave B appeared larger in experiments employing a 10 s holding time immediately after traversing wave A. These observations indicate that wave B arises from the reversible reduction of the rhodocenium complex generated at wave A. The events giving rise to the cyclic voltammetry of **9a** are depicted in Scheme 2.

Exhaustive bulk electrochemical oxidation of **9a** was accomplished by poising the working electrode potential at +0.15 V. The electrolysis required 1.1 F/mol to come to completion and caused the originally yellow solution to become colorless. CV scans obtained after electrolysis

(10) For a discussion of homogeneous reactions following heterogeneous electron transfer, see: Bard, A. J.; Faulkner, L. R. *Electrochemical Methods*; Wiley: New York, 1980; pp 429−487.

Scheme 2

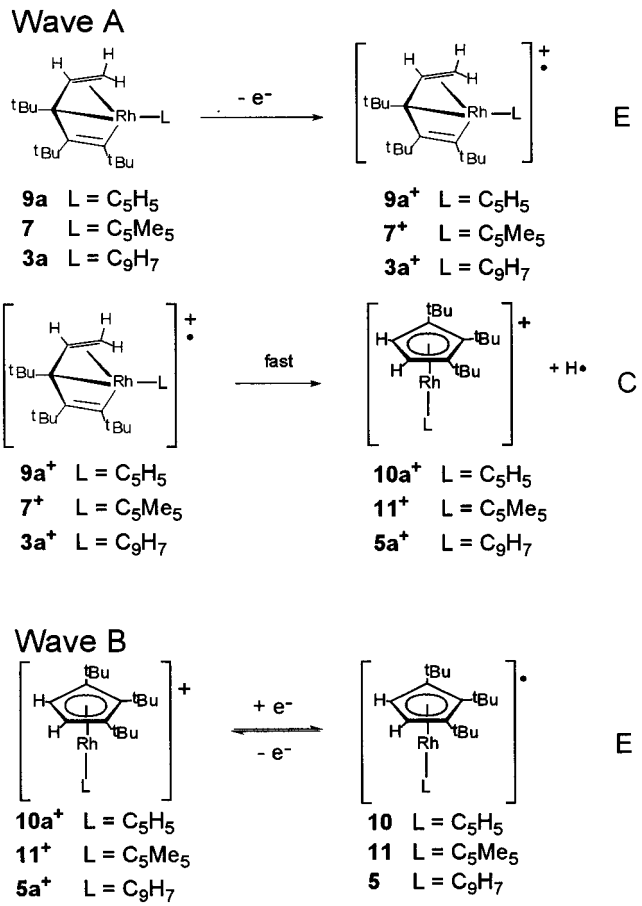

show the absence of wave A and the presence of wave B regardless of the initial scan direction.

Oxidation of **9a** was also accomplished by chemical means, using 1 equiv of ferrocenium hexafluorophosphate as the oxidizing agent. The product of the chemical oxidation was identified unambiguously as rhodocenium complex **10a**$^+$ by NMR spectroscopy and the results of a single-crystal X-ray diffraction study. The ^{1}H NMR spectrum (CD_3CN solution) displays singlets at 1.45 ppm (18H) and 1.56 ppm (9H) for the lateral and central *tert*-butyl groups, respectively, of the substituted cyclopentadienyl ligand. A singlet at 5.85 ppm (2H) is assigned to the two ring protons of the tri-*tert*-butylcyclopentadienyl ligand. Likewise, the singlet at 5.89 ppm (5H) is assigned to the five protons of the unsubstituted cyclopentadienyl ligand. The cyclic voltammetry of **10a**$^+$ in THF solution (Figure 2) is characterized by a wave of limited chemical reversibility at $E_{1/2}$ = −1.83 V.[9] This is the same potential observed for wave B in the voltammetry of both **9a** and the product of electrochemical oxidation of **9a**. Similar results were obtained when **9a** was treated with ferrocenium tetrafluoroborate.

X-ray Diffraction Studies of 10a$^+$ and 10b$^+$. The solid-state structures of **10a**$^+$ and **10b**$^+$ were determined by the results of single-crystal X-ray diffraction studies. The crystallographic data for these complexes are listed in Table 1. Figure 3 displays an ORTEP plot of the cationic portion of the tetrafluoroborate salt **10b**$^+$. Selected bond distances and angles for **10b**$^+$ are provided in Figure 4. The structure assumes a sandwich arrangement with both rings binding to the metal in

Table 1. Crystallographic Data for $10a^+$ and $10b^+$

	$10a^+$	$10b^+$
formula	$C_{22}H_{34}F_6PRh$	$C_{22}H_{34}BF_4Rh$
fw	546.37	488.21
space group	$P6_3/m$	$P2_1/c$
a, Å	28.185(12)	13.398(6)
b, Å		15.400(3)
c, Å	15.532(3)	10.754(4)
β, deg		100.35(3)
V, Å^3	10685(7)	2183.0(16)
Z	18	4
crystal color, habit	light brown prism	colorless block
D(calc), g cm^{-3}	1.528	1.486
μ(Mo Kα), cm^{-1}	8.40	8.20
temp, K	298(2)	243(2)
diffractometer	Siemens P4	Siemens P4
$R(F)$, %[a]	7.64	5.54
$R_w(F)$, %[a]	9.19	
$R_w(F^2)$, %[b]		14.36

[a] Quantity minimized = $\sum\Delta^2$; $R = \sum\Delta/\sum(F_o)$; $R_w = \sum\Delta w^{1/2}/\sum(F_o w^{1/2})$, $\Delta = |(F_o - F_c)|$. [b] Quantity minimized = $R_w(F^2) = \sum[w(F_o^2 - F_c^2)^2]/\sum[w(F_o^2)^2]^{1/2}$; $R = \sum\Delta/\sum(F_o)$, $\Delta = |(F_o - F_c)|$.

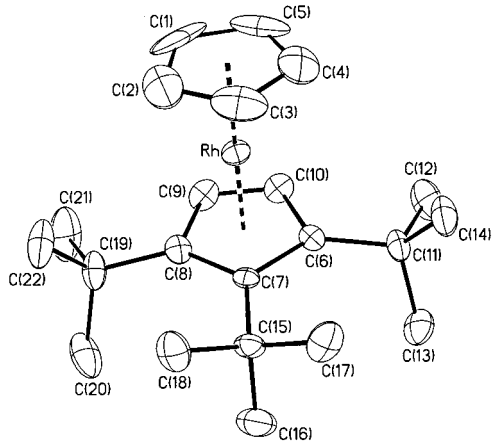

Figure 3. ORTEP plot of the cationic portion of $\mathbf{10b}^+$.

an η^5 fashion. The angle between the Rh−ring centroid vectors is 177.2°. The Rh−centroid distance of the substituted ligand (1.795 Å) is slightly shorter than the analogous distance of the unsubstituted cyclopentadienyl ligand (1.819 Å), which can be attributed to the greater inductive effect of the ^{t}BuCp ligand vs that of the C_5H_5 ligand. The cyclopentadienyl ligands are positioned in an eclipsed conformation.

The presence of *tert*-butyl groups on adjacent carbon atoms of the substituted cyclopentadienyl ligand in $\mathbf{10b}^+$ raises the question of whether the steric repulsion of the *tert*-butyl substituents will result in any deformations of the molecule. Both rings are nearly planar; out-of-plane displacement of the *tert*-butyl substituents is not observed. The steric strain in the molecule is apparently relieved by in-plane deformation of the bond lengths and angles of the tri-*tert*-butylcyclopentadienyl ligand. The bond angles of the ring differ from 108°, the value expected for a pentagon. The bond angles C(9)−C(8)−C(7) (106.7°), C(8)−C(7)−C(6) (107.0°), and C(7)−C(6)−C(10) (105.8°), where each of the central carbon atoms contains a *tert*-butyl substituent, are somewhat smaller than 108°, presumably to allow more room between adjacent *tert*-butyl groups. As a result, the remaining angles of the ring are somewhat larger than 108°. The bond lengths between the ring carbon atoms bearing *tert*-butyl substituents are longer than

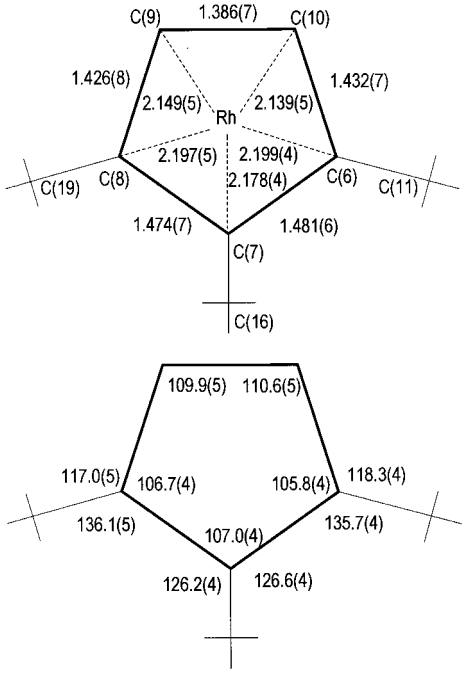

Figure 4. Selected bond lengths (Å) (top) and bond angles (deg) (bottom) for the substituted cyclopentadienyl ligand of complex $\mathbf{10b}^+$.

the value of approximately 1.40 Å observed for rhodium complexes containing cyclopentadienyl ligands.[11] The bond angles (C(7)−C(6)−C(11) and C(7)−C(8)-C(19)) involving the lateral *tert*-butyl substituents are significantly larger than the analogous bond angles (C(16)−C(7)−C(6) and C(16)−C(7)−C(8)) encompassing the central *tert*-butyl group. These observations are in agreement with the results of the previously reported crystal structure of $\mathbf{5a}^+$.[4b]

$\mathbf{10a}^+$ cystallizes in the hexagonal space group, $P6_3/m$, with three symmetry-independent cations (Figure 5), each situated on a crystallographic mirror plane ($^1/_2$ occupancy), and four independent hexafluorophosphate anions, with one on a $\bar{3}$ site ($^1/_6$ occupancy), one on a 3-fold site ($^1/_3$ occupancy), and two on mirror planes. The ring systems on Rh(1) are perfectly eclipsed, on Rh(3) perfectly staggered, and on Rh(2) perfectly disordered. The disorder was modeled approximately as a hexagon with $^5/_6$ occupancy carbon and hydrogen atoms but appears to be more nearly a featureless torus of electron density. Selected bond distances and angles are given in Figures 6 and 7, respectively, and in Table 2. The three cations are bent such that the planes open slightly on the substituted side; the centroid−Rh−centroid angles vary from 175.7 to 177.1°. As with $\mathbf{10b}^+$, the Rh−centroid distances are somewhat shorter to the substituted ring (average 1.78 Å) as compared to the unsubstituted ring (average 1.83 Å). Both rings are planar and bind to the metal in an η^5 manner. The tri-*tert*-butylcyclopentadienyl ligand experiences in-plane distortions similar to those described for $\mathbf{10b}^+$ and $\mathbf{5a}^+$ [4b] apparently to relieve the steric strain imposed on the molecule by the adjacent *tert*-butyl substituents.

(11) For examples, see: (a) Bruce, M. I.; Rodgers, J. R.; Walton, K. *J. Chem. Soc., Chem. Commun.* **1981**, 1253. (b) Restivo, R.; Ferguson, G.; O'Sullivan, D. J.; Lalor, F. J. *Inorg. Chem.* **1975**, *14*, 3046. (c) Cash, G. C.; Helling, J. F.; Matthew, M.; Palenik, G. J. *J. Organomet. Chem.* **1973**, *50*, 277.

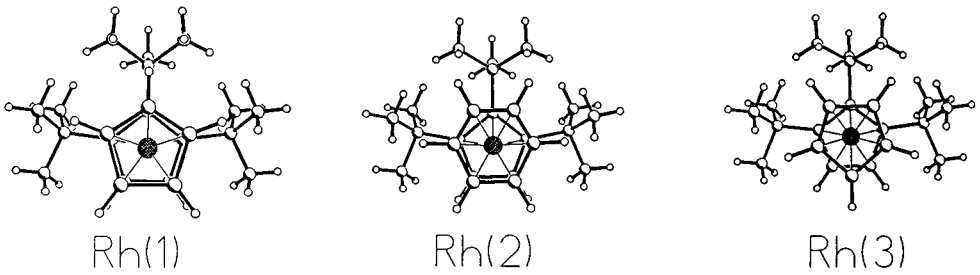

Figure 5. Comparison of the three crystallographically independent cations of **10a**$^+$. At Rh(1) the rings are eclipsed, at Rh(2) the unsubstituted ring is rotationally disordered and approximately modeled as a six-membered ring, and at Rh(3) the rings are staggered.

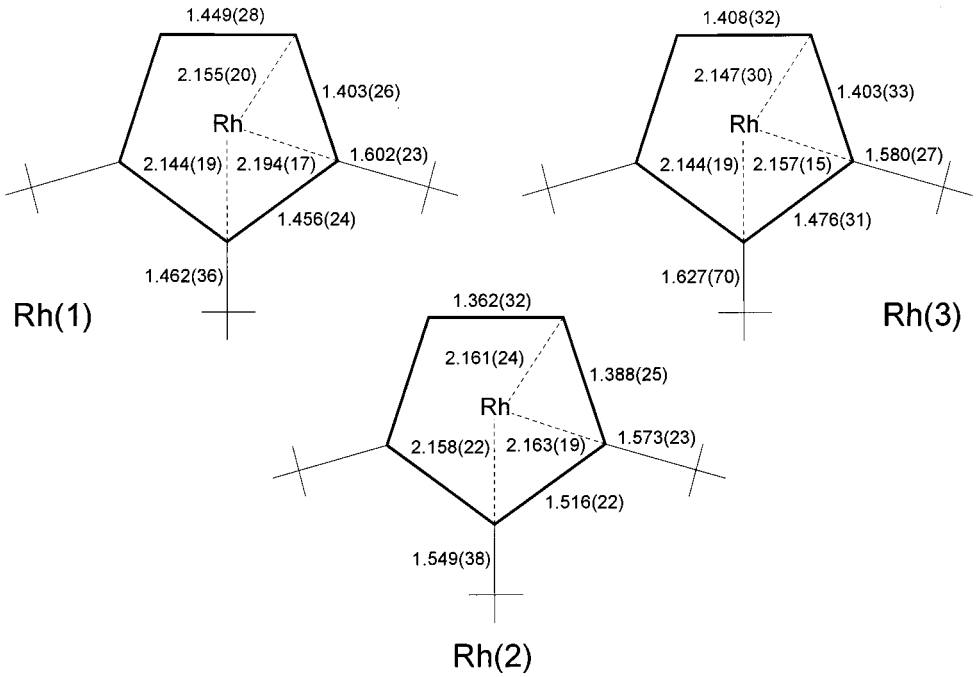

Figure 6. Selected bond distances (Å) for the substituted cyclopentadienyl ligands of the three crystallographically independent cations of **10a**$^+$.

(ii) The Pentamethylcyclopentadienyl Complex, 7. A typical CV scan of **7** is shown in Figure 8. Initiation of the scan in the positive potential direction reveals a chemically irreversible oxidation wave (labeled A) at $E_{p_a} = -0.10$ V. Reversal of the scan direction after traversing wave A shows three small chemically irreversible reduction waves (labeled C, D, and E) and a much larger chemically reversible reduction wave labeled B at $E_{1/2} = -2.03$ V. Waves B−E are only observed when wave A is traversed first. Additionally, wave B shows a considerable increase in current height when a 10 s delay is imposed immediately after scanning through wave A. We will demonstrate that wave A arises from a 1 e$^-$ chemically irreversible oxidation of **7** to form rhodocenium complex **11**$^+$ and that wave B arises from the reduction and reoxidation of **11**$^+$.[12]

Exhaustive electrochemical oxidation of **7** was conducted by applying a potential of −0.04 V to a platinum basket working electrode. The electrolysis required 0.92 F/mol and caused the solution to change from orange to dark pink-orange. A cyclic voltammetry scan obtained after electrolysis is shown in Figure 9. The absence of wave A indicates complete consumption of **7**.

Two chemically reversible waves are present, a small one at $E_{1/2} = +0.15$ V (wave F) and a larger one at $E_{1/2} = -2.04$ V (wave B). Waves B and F are present regardless of the direction in which the CV scan is initiated, indicating that one wave is not a product of the other. Wave F was determined to be due to the chemically reversible oxidation of η^4-cyclobutadienyl complex **8** by synthesizing the compound according to the literature procedure[6] and investigating its cyclic voltammetry behavior: the authentic sample displays a chemically reversible wave at $E_{1/2} = +0.15$ V, which matches the half-wave potential of wave F.

To identify the process giving rise to wave B, a sample of **7** was treated with 1 equiv of ferrocenium hexafluorophosphate. The product was identified as rhodocenium complex **11**$^+$ on the basis of ^{1}H NMR data obtained from a $CDCl_3$ solution of the compound. Singlets observed at 1.45 ppm (18H) and 1.50 ppm (9H) were assigned to the lateral and central *tert*-butyl groups, respectively, of the tri-*tert*-butylcyclopentadienyl ligand; a singlet at 2.07 ppm (15H) was assigned to the methyl protons of the pentamethylcyclopentadienyl ligand. The

(12) Wave B is completely chemically reversible at all scan rates employed (50−1000 mV/s). We are currently investigating the consequences of reducing **11**$^+$ in bulk electrolysis experiments.

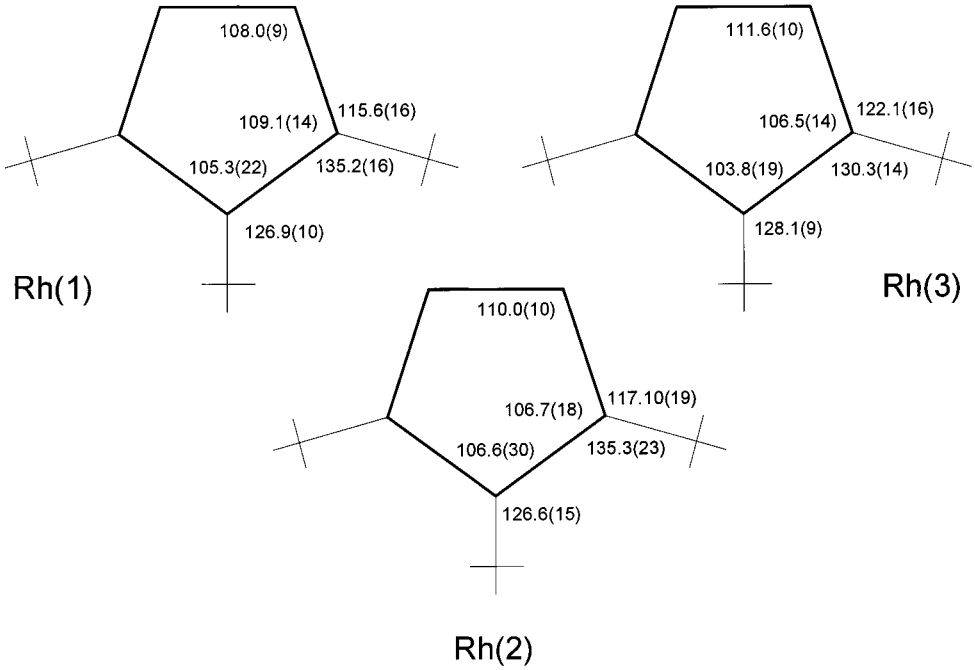

Figure 7. Selected bond angles (deg) for the substituted cyclopentadienyl ligands of the three crystallographically independent cations of **10a**$^+$.

Table 2. Selected Bond Distances (Å) and Angles (deg) for 10a$^+$

	mol A (Rh1)	mol B (Rh2)	mol C (Rh3)
ct (C_5H_5)−Rh[a]	1.82(1)	1.83(1)	1.83(1)
ct ($C_5{}^tBu_3H_2$)−Rh	1.79(1)	1.78(1)	1.76(1)
ct−Rh−ct	176.5(8)	175.7(8)	177.1(9)
C_5 planes, dihedral	5.1	3.3	2.3

[a] ct = centroid.

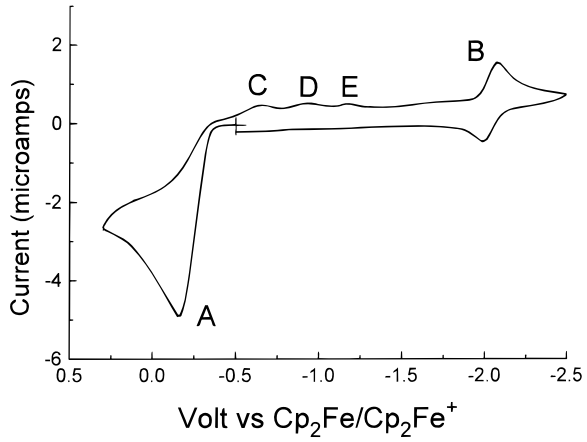

Figure 8. Cyclic voltammetry scan of 0.99 mM **7** in THF solution. The scan was initiated in the positive potential direction. The lettered waves arise from the following reactions: (A) **7** ⇔ **11**$^+$ + e$^-$; (B) **11**$^+$ + e$^-$ ⇔ **11**. A platinum disk working electrode was used with scan rate = 200 mV/s. The scan was initiated in the positive potential direction.

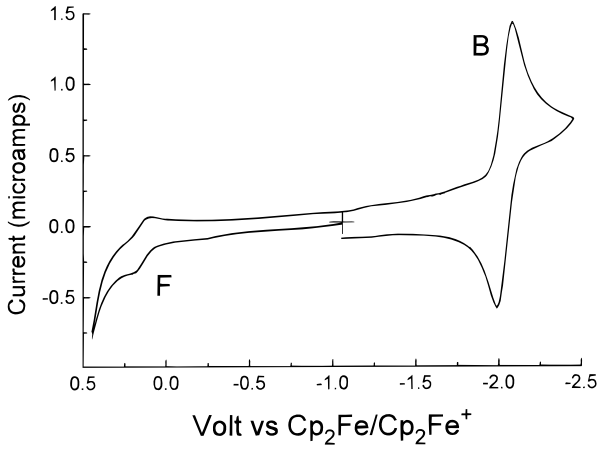

Figure 9. Cyclic voltammetry scan obtained after exhaustive electrochemical oxidation of 0.5 mM **7** in THF solution. The lettered waves arise from the following processes: (B) **11**$^+$ + e$^-$ ⇔ **11**; (F) **8** ⇔ **8**$^+$ + e$^-$. A platinum disk electrode was employed with scan rate = 200 mV/s. The scan was initiated in the positive potential direction.

remaining signal in the spectrum, a singlet at 5.89 ppm (2H), was assigned to the two equivalent protons of the tri-*tert*-butylcyclopentadienyl ligand. Cyclic voltammetry scans of **11**$^+$ in THF solution show the presence of a chemically reversible wave at $E_{1/2} = -2.04$ V, the same potential observed for wave B in CV scans obtained before and after oxidation of **7**. Hence rhodocenium complex **11**$^+$ is produced by chemical or electrochemical oxidation of **7**. The electrochemical conversion **7** → **11**$^+$ is described in Scheme 2.

(iii) The Indenyl Derivative, 3a. Typical CV scans of **3a** are shown in Figures 10 and 11.

The scan in Figure 10 was initiated in the positive potential direction whereas the scan in Figure 11 was initiated in the negative potential direction. A comparison of the two voltammograms aids in understanding the electrochemistry of the compound. We turn our attention first to Figure 11, which shows the simpler of the two voltammograms. Wave D arises from a chemically irreversible *reduction* of **3a**; this wave is present regardless of whether any other waves have been traversed first. Waves E and F appear only when D has been scanned first and hence are products of D.[13] Turning now to Figure 10, we see that waves A, G, B, and C are present in addition to waves D, E, and F.

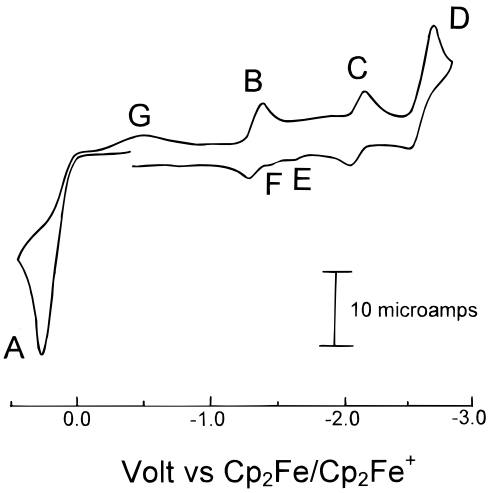

Figure 10. Cyclic voltammogram of 1.53 mM **3a** obtained in THF solution. The scan was initiated in the *positive* potential direction. Conditions: platinum disk working electrode; scan rate = 200 mV/s.

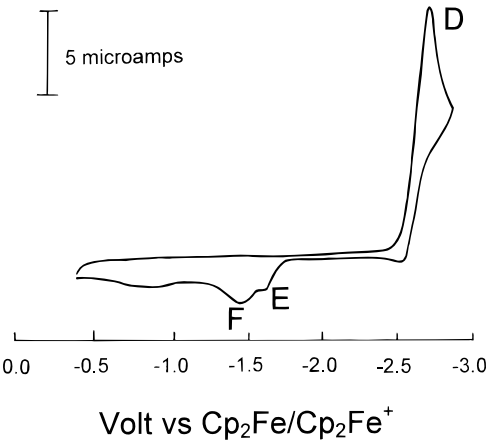

Figure 11. Cyclic voltammogram of 1.53 mM **3a** obtained in THF solution. The scan was initiated in the *negative* potential direction. Conditions: platinum disk working electrode; scan rate = 200 mV/s.

Wave A (E_{p_a} = +0.28 V) arises from a chemically irreversible oxidation of **3a**. Waves G, B ($E_{1/2}$ = −1.41 V) and C ($E_{1/2}$ = −2.17 V) are only observed after wave A has been traversed first. We will demonstrate that oxidation of **3a** at wave A affords **5a**$^+$.

3a was oxidized electrochemically by holding the working electrode potential at +0.50 V. The electrolysis required 1.33 F/mol and caused the solution to change from orange-red to bright yellow. Figure 12 shows a typical CV scan obtained after electrolysis. The absence of wave A indicates complete consumption of **3a** during the course of the electrolysis. The major waves present after electrolysis are B and C, which have $E_{1/2}$ values identical to those of waves B and C of Figure 10. These waves arise from sequential one-electron reductions of rhodocenium complex **5a**$^+$ (vide infra). Waves H, I, and J probably arise from redox events of minor products generated during the electrolysis.

The reaction of **3a** with 1 equiv of ferrocenium tetrafluoroborate produced rhodocenium complex **5c**$^+$.

(13) The consequences of reducing **3a** are currently under investigation in our laboratory.

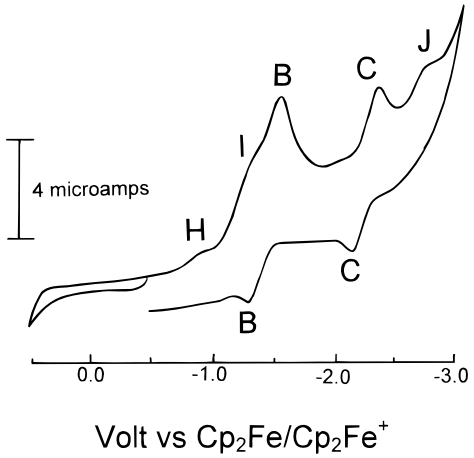

Figure 12. Cyclic voltammogram obtained after bulk electrochemical oxidation of 0.86 mM **3a** in THF solution. Conditions: platinum disk woking electrode; scan rate = 200 mV/s. The scan was initiated in the positive potential direction.

The ^{1}H NMR data of the product matched those reported in the literature.[4b] A CV scan of **5c**$^+$ in THF solution shows the presence of two chemically reversible waves having $E_{1/2}$ values identical to those of waves B and C in Figure 10. Scheme 2 describes the events giving rise to waves A and B in the electrochemistry of **3a**. At wave A, the complex undergoes a chemically irreversible oxidation to form rhodocenium complex **5a**$^+$. The rhodocenium complex then undergoes a chemically reversible reduction at wave B to form the neutral rhodocene compound **5**. At wave C, **5** undergoes further reduction.[14]

II. Deuterium-Labeling Study of the Ring-Closure Reaction. The stereochemistry of the redox-induced ring-closure reaction was probed by examining the consequences of oxidizing deuterium-labeled isotopomer **9b** in which deuterium is located exclusively in the syn position of the pentadienediyl ligand. Reaction of **9b** with a stoichiometric amount of ferrocenium hexafluorophosphate afforded **10c**$^+$ which was identified and shown to contain deuterium on its tri-*tert*-butylcyclopentadienyl ring by ^{1}H and ^{2}H NMR studies. A ^{1}H NMR spectrum of **10c**$^+$ in $CDCl_3$ solution displays singlet resonances at 1.46 ppm (18H) and 1.55 ppm (9H) which are assigned to the lateral and central *tert*-butyl groups, respectively, of the tri-*tert*-butylcyclopentadienyl ligand. The singlet appearing at 5.87 ppm (5H) is assigned to the protons of the unsubstituted cyclopentadienyl ligand; the remaining singlet at 6.01 ppm (1H) is attributed to the ring proton of the substituted cyclopentadienyl ligand. The ^{2}H NMR spectrum displays only one singlet at 6.03 ppm, indicating the presence of deuterium on the substituted cyclopentadienyl ligand. Apparently, the redox-promoted ring-closure reaction proceeds with the same stereochemistry found for the thermally promoted ring-closure reaction of indenyl derivative **3b** (see Figure 1).[4a]

III. Computational Studies of the Ring-Closure Reaction. Several model rhodium organometallic complexes were studied using the PM3 semiempirical

(14) We are currently studying the consequences of reducing **5a**$^+$ in more detail. It is possible that the indenyl ligand of electrogenerated rhodocene **5** may undergo ring slippage to form an η^3-indenyl complex.

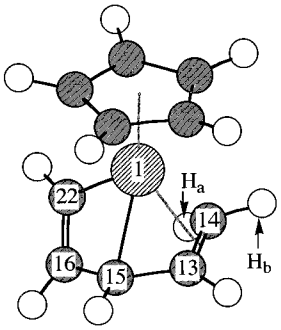

Rh(1)-C(13) = 2.17 (2.10)
Rh(1)-C(14) = 2.12 (2.14)
Rh(1)-C(15) = 2.16 (2.20)
Rh(1)-C(22) = 2.05 (2.11)
C(13)-C(14) = 1.46 (1.40)
C(15)-C(16) = 1.50 (1.53)
C(16)-C(22) = 1.34 (1.35)
C(13)-C(15) = 1.44 (1.42)
Rh(1)...Cp = 1.82 (1.94)

A

ΔH_f(PM3) = -259.935 kcal mol^{-1}

Figure 13. Calculated structure **A**, showing selected bond distances and ΔH_f(PM3).

Hamiltonian after calibration of the method by comparison of known and predicted structures for prototypical rhodium complexes.[15] An extensive survey of over 40 plausible complexes with formula CpRh(C_5H_6) yielded two structures that have calculated energies significantly (i.e., ≥4 kcal mol^{-1}) lower than all others. Calculated structure **A** (CpRh(pentadienediyl)) (see Figure 13) is in very good agreement with experimental structure **9a** and is 0.5 kcal mol^{-1} more stable than the other low-energy isomer, CpRh(η^4-cyclopentadiene).

It is of interest to probe the molecular and electronic structural consequences resulting when complexes such as **9a** are converted to rhodocenium derivatives by oxidation. Removal of an electron from **A** followed by geometry optimization resulted in radical cation $\mathbf{A}^{+\bullet}$. The change in the geometry of the C_5H_6 moiety upon oxidation of **A** to $\mathbf{A}^{+\bullet}$ hinted of incipient ring closure; this group became more planar, and the distance between nonbonded carbons (C(22) and C(14)) decreased from 2.76 Å (**A**) to 2.60 Å ($\mathbf{A}^{+\bullet}$). The changes in geometry of the pentadienediyl ligand upon oxidation of **A** suggest that the electron is removed from a molecular orbital (MO) centered on the C_5H_6 (pentadienediyl) ligand. This inference is supported by the observation that the two highest MOs in **A** are centered on the C_5H_6 ligand and that the majority of the spin density in $\mathbf{A}^{+\bullet}$ is located on the C_5H_6 ligand.[16]

Conclusions

The results presented herein demonstrate that although their thermally promoted reactions differ greatly from one another, pentadienediyl complexes **3**, **7**, and **9** all undergo single-electron oxidation to afford rhodocenium complexes bearing the novel 1,2,3-tri-*tert*-butylcyclopentadienyl ligand. Oxidation of deuterium-labeled isotopomer **9b** revealed that the stereochemistry of the redox-induced ring-closure reaction $\mathbf{9b}^+ \rightarrow \mathbf{10c}^+$ studied in this work is in agreement with the thermally induced ring-closure reaction $\mathbf{3a} \rightarrow \mathbf{5a}^+$ reported by Hughes and co-workers.[4a] We are currently investigating the redox-induced reactions of other rhodium pentadienediyl complexes and the consequences of reducing the rhodocenium complexes $\mathbf{5}^+$, $\mathbf{10}^+$, and $\mathbf{11}^+$. The results of these studies will be reported in due course.

Experimental Section

Synthetic Procedures and Chemicals. All reactions were conducted in oven-dried glassware under a dinitrogen atmosphere using either standard Schlenk or glovebox techniques unless otherwise noted. Solvents were distilled from the appropriate drying agents (potassium metal for tetrahydrofuran, diethyl ether, and petroleum ether (bp 30−60 °C); 4 Å molecular sieves for acetone; calcium hydride for methylene chloride) immediately prior to use. Compounds **1a**,[7] **2**,[7] **3a**,[4] **7**,[6] and **9a**[7] were prepared according to the literature methods. Ferrocenium hexafluorophosphate and ferrocenium tetrafluoroborate were prepared by treating ferrocene with silver hexafluorophosphate or silver tetrafluoroborate, respectively, in acetone solution.[17] Tetrabutylammonium hexafluorophosphate, purchased from Southwest Analytical Chemicals, was recrystallized from acetone three times and dried under vacuum for 24 h prior to use. Silica gel (Davisil 62) was purchased from Mallinckrodt and used as received. ^{1}H, ^{2}H, and ^{13}C NMR data were obtained at 300.197, 46.082, and 75.582 MHz, respectively, using a General Electric QE-300 Spectrometer modified with a Tecmag Aquerius software upgrade.

Electrochemical Procedures. Electrochemical studies were performed on an EG&G Princeton Applied Research (PAR) model 273 potentiostat/galvanostat driven using the EG&G model 270/250 research electrochemistry software package. All electrochemistry experiments were conducted in an Mbraun Lab Master 100 glovebox. Experiments employed a conventional three-electrode configuration. A Luggin capillary probe for the reference electrode (Ag/AgCl of SCE) and positive-feedback *iR* compensation were used routinely in voltammetry experiments. In bulk electrolysis experiments, the auxiliary (platinum mesh) and reference electrodes were separated from the working electrode compartment by fine sintered glass frits. The applied potential was held at the value specified until the current decayed to less than 5% of its original value. All potentials are referenced to the ferrocene/ferrocenium redox couple, used as an internal standard; this redox couple has an $E_{1/2}$ value of +0.56 V vs SCE under the same experimental conditions employed in this study (tetrahydrofuran solution containing 0.1 M tetrabutylammonium hexafluorophosphate).

The cyclic voltammetry of **3a**, **7**, and **9a** was investigated in tetrahydrofuran solution using either glassy carbon, platinum, or gold disk working electrodes. The voltammetry responses of the compounds were unaffected by the choice of electrode material. Linear plots of peak potential vs (scan rate)$^{1/2}$ were obtained for the oxidation wave of each of the compounds (wave A in Figures 1, 8, and 10), indicating diffusion control of mass transfer.

Reaction of 9a with $FcPF_6$. **9a** (0.334 g, 0.829 mmol) and ferrocenium hexafluorophosphate (0.284 g, 0.858 mmol) were allowed to react in acetone (25 mL) solution under a nitrogen atmosphere for 1 h. After removal of the solvent under reduced pressure, the product was purified in the air by

(15) Calculations were performed using the program MacSpartan Plus (Wavefunction Inc., Irvine, CA, 1996) and the PM3 semiempirical Hamiltonian. The PM3 method is described in: Stewart, J. J. P. *J. Comput.-Aided Mol. Des.* **1990**, *4*, 1.

(16) Although this computational investigation does not indicate that an η^4-cyclopentadiene complex actually forms as a result of removing an electron from CpRh(C_5H_6), it should be pointed out that electrochemical oxidation of an η^4-cyclopentadiene rhodium complex results in loss of H$^\bullet$ and formation of an η^5-cyclopentadienyl complex. See: Ustynyuk, N. A.; Pererleitner, M. G.; Gusev, O. V.; Denisovich, L. I. *Russ. Chem. Bull.* **1993**, 1727. For an analogous reaction involving an (η^4-pentamethylcyclopentadiene)platinum complex, see: Gusev, O. V.; Morozova, L. K.; Peganova, T. A.; Peterleitner, M. G.; Peregudova, S. M.; Denisovich, L. I.; Petroskii, P. V.; Oprunenko, Y. F.; Ustynyuk, N. A. *J. Organomet. Chem.* **1995**, *493*, 181.

(17) For an excellent review on chemical redox reagents, see: Connelly, N. G.; Geiger, W. E. *Chem. Rev.* **1996**, *96*, 877.

chromatography on a silica gel column (5.5 cm × 2.54 cm) packed in petroleum ether (bp 30−60 °C). The product was introduced into the column by dissolving it in a minimum of methylene chloride. Ferrocene was removed from the column by elution with petroleum ether. Once the eluent became completely colorless, acetone was introduced into the column, resulting in elution of **10a**$^+$. Solvent was removed under reduced pressure to afford 0.342 g of **10a**$^+$ as a tan solid (78% yield). An analytically pure sample was obtained by adding 0.6 mL of chloroform to 0.0770 g of the product and sonicating the resulting mixture at 45 °C. This left a brown insoluble product at the bottom of the flask. The colorless solution was decanted into a clean flask. Solvent was removed, leaving a white powder. Yield (based on crude product): 0.038 g (50%). Anal. Calcd for $C_{22}H_{34}F_6PRh$: C, 48.36; H, 6.27. Found: C, 48.39; H, 6.33. Crystals suitable for single-crystal X-ray analysis were obtained by vapor diffusion of diethyl ether into a saturated solution of **10a**$^+$ (obtained from chromatographic purification) in methanol. ^{1}H NMR (acetone-d_6): δ 1.53 (s, 18H, ^{t}Bu), 1.64 (s, 9H, ^{t}Bu), 6.09 (s, 2H, $C_5{}^t$Bu$_3H_2$), 6.19 (s, 5H, C_5H_5). ^{1}H NMR (CD_3CN): δ 1.45 (s, 18H, ^{t}Bu), 1.56 (s, 9H, ^{t}Bu), 5.85 (s, 2H, $C_5{}^t$Bu$_3H_2$), 5.89 (s, 5H, C_5H_5). ^{13}C{^{1}H} NMR (acetone-d_6): δ 33.71 (s), 34.72 (s), 35.39 (s), 35.62 (s), 86.31 (d, J_{Rh-C} = 9.7 Hz), 88.64 (d, J_{Rh-C} = 7.3 Hz), 118.30 (d, J_{Rh-C} = 7.3 Hz), 123.42 (d, J_{Rh-C} = 9.7 Hz).

Reaction of 9a with FcBF$_4$. 9a (0.231 g, 0.573 mmol), ferrocenium tetrafluoroborate (0.165 g, 0.603 mmol), and acetone (25 mL) were added to a Schlenk flask. After the resulting mixture was allowed to stir for 1 h, solvent was removed under reduced pressure. The product was dissolved in a minimum amount of methylene chloride, and the solution was placed on a silica gel column (6 cm × 2.5 cm) packed in petroleum ether. After removal of all of the ferrocene from the column by elution with petroleum ether, the desired product was eluted using acetone. Removal of the solvent afforded **10b**$^+$ (0.230 g, 82% yield). The product was then twice recrystallized from chloroform as described for **10a**$^+$ to obtain white crystals (0.091 g, 33% based on the amount of **9b** used). ^{1}H NMR ($CDCl_3$): δ 1.46 (s, 18H, lateral ^{t}Bu), 1.55 (s, 9H, central ^{t}Bu), 5.87 (s, 2H, $C_5{}^t$Bu$_3H_2$), 6.01 (s, 5H, C_5H_5). Crystals suitable for single-crystal X-ray analysis were obtained by dissolving some of the solid in acetone-d_6 and allowing the solvent to evaporate over the course of 4 months.

Reaction of 9b with FcPF$_6$. 9b (30 mg, 0.074 mmol), ferrocenium hexafluorophosphate (25 mg, 0.074 mmol) and acetone (10 mL) were combined in a Schlenk flask. After the mixture was allowed to stir for 1 h, solvent was removed. The residue was chromatographed on silica gel packed in petroleum ether. Ferrocene was removed from the column by elution with petroleum ether. **10c**$^+$ was eluted with acetone. Removal of the solvent afforded an off-white powder. ^{1}H NMR ($CDCl_3$): δ1.46 (s, 18H, ^{t}Bu), 1.55 (s, 9H, ^{t}Bu), 5.87 (s, 5H, C_5H_5), 6.01 (s, 1H, $C_5{}^t$Bu$_3H$D). ^{2}H NMR ($CHCl_3$): δ 6.03 (s, 1D, $C_5{}^t$Bu$_3$H*D*).

Reaction of 7 with FcPF$_6$. Acetone (15 mL) was added to a mixture of **7** (0.090 g, 0.188 mmol) and ferrocenium hexafluorophosphate (0.069 g, 0.201 mmol) in a Schlenk flask. The resulting mixture was allowed to stir at room temperature for 2 h. After removal of solvent, the product was chromatographed on a silica gel column (14.5 cm × 1.5 cm) packed in petroleum ether. After removal of ferrocene from the column using petroleum ether, the rhodocenium complex was eluted with acetone. Evaporation of the solvent afforded a tan powder (0.049 g, 0.008 mmol, 41%). ^{1}H NMR ($CDCl_3$): δ 1.45 (s, 18H, ^{t}Bu), 1.50 (s, 9H, ^{t}Bu), 2.07 (s, 15H, C_5Me_5), 5.89 (s, 2H, $C_5{}^t$Bu$_3H_2$).

Reaction of 3a with FcBF$_4$. 3a (0.156 g, 0.344 mmol), ferrocenium tetrafluoroborate (0.108 g, 0.94 mmol), and acetone (15 mL) were placed in a Schlenk flask under a nitrogen atmosphere, and the resulting solution was allowed to stir for 30 min. The volume was then reduced in vacuo to ca. 1−2 mL to obtain a viscous brown solution. The residue was rinsed with petroleum ether to remove ferrocene. Recrystallization of the product from acetone afforded bright yellow crystals of **5c**$^+$ (0.076 g, 41% yield based on the original amount of **3a** used). A ^{1}H NMR spectrum obtained in $CDCl_3$ solution matched the literature spectrum.[4b]

Crystallographic Structural Determination. Crystal, data collection, and refinement parameters for **10a**$^+$ and **10b**$^+$ are given in Table 1.

The systematic absences in the diffraction data were consistent for space groups $P6_3$ and $P6_3/m$ for **10a**$^+$ and were uniquely consistent for space group $P2_1/c$ for **10b**$^+$. In the case of **10a**$^+$, the latter centrosymmetric space group was preferred on the basis of the chemically reasonable and computationally stable results of refinement. The structures were solved using direct methods, completed by subsequent difference Fourier synthesis and refined by full-matrix least-squares procedures. The absorption corrections were not required because the variation in the integrated ψ-scan intensities was less than 10% for both **10a**$^+$ and **10b**$^+$.

The asymmetric unit of **10a**$^+$ consists of three independent cations residing on mirror planes and four independent anions (two on mirror planes, one on a 3-fold axis, and one on a 3-fold inversion axis). Due to limited data, anisotropic refinement was confined to the Rh, P, and F atoms. Disorder in one of the Cp rings on Rh(2) is described in the text. In addition, one of the anions is axially disordered about P(1) which, due to its presence on a 3-fold inversion site, contains an equatorial plane with six F atoms, instead of four, each refined with $^2/_3$ occupancy. For **10b**$^+$, all non-hydrogen atoms were refined with anisotropic displacement coefficients. In both structures all hydrogen atoms were treated as idealized contributions.

All software and sources of the scattering factors are contained in SHLXTL (version 5.03) and various versions of the SHLXTL PC and VAX program library (G. Sheldrick, Siemens XRD, Madison, WI).

Acknowledgment. B.T.D.-M. is grateful to the donors of the Petroleum Research Fund, administered by the American Chemical Society, and The University of North Carolina at Charlotte for generous financial support of this research and to Professor Russell P. Hughes for providing a sample of **2b**. T.R.C. acknowledges the National Science Foundation for support (Grant CHE-9614346).

Supporting Information Available: Tables of crystal data, structure refinement details, atomic coordinates, bond distances, bond angles, and thermal parameters (18 pages). Ordering information is given on any current masthead page.

OM9707735